

Operational Modal Analysis of Rotating Machinery

S. Gres², P. Andersen¹, and L. Damkilde²

¹ Structural Vibration Solutions A/S, NOVI Science Park, Niels Jernes Vej 10, Aalborg, DK 9220,

² Department of Civil and Structural Engineering, Aalborg University, Thomas Manns Vej 23, Aalborg, DK 9000,

ABSTRACT

Harmonic excitation of structures caused by rotating equipment is a problem faced by many engineers in the field of Operational Modal Analysis (OMA). Several methods to discard the influence of harmonic inputs over systems natural responses has been proposed in the literature and implemented in various software solutions. This paper recalls some of the most used techniques and uses a new time domain method for removing harmonics from measurements. Deployed method does not rely on filtering, statistical detection nor on non-linear fitting. Instead, it predicts the harmonic part of the time series and deploys an orthogonal projection of the latter onto the raw measurements to remove the harmonic part of the signal. The new technique is a part of an semi-automated framework for OMA of structures contaminated with harmonics, whose flow is presented in this paper. The merit of the framework is discussed in the context of OMA of a full scale operating ship with rotating machinery on-board.

Keywords: Operational Modal Analysis, Rotating Machinery, Harmonic Removal, Harmonic Detection, Stochastic Subspace Identification

1 INTRODUCTION

In the context of OMA of rotating machinery, that is estimation of natural frequencies, damping ratios and mode shapes of structures subjected to both harmonic and random excitations based only on the response measurements, a couple of schemes has been proposed. As such, each strategy that deals with harmonic disturbances in OMA consists of a common triad: harmonic detection, harmonic removal and system parameter computation.

In that context Peeters et al. [1] presented a scheme of time-synchronous-averaging (TSA) and polyreference least-squares complex frequency-domain method (PolyMAX) that was used for OMA of an steady-flight helicopter and an operating diesel engine. Deployed duo enabled OMA of harmonic-affected signals by removing the harmonic peaks from an auto spectral densities of the measurement channels what improved clarity of the estimated stabilization diagrams. For a non-stationary harmonics the TSA required an tachometer measurements from rotating components for angular resampling, which is most often not recorded in real-life application; that was attempted to overcome by Combet and Gelman [2].

An alternative strategy for OMA of rotating machinery is based on cepstral methods. Cepstrum is an inverse Fourier transform of the logarithm of the spectrum which real part is deployed in the recent studies by Randall and Smith [3] and Randall et al. [4] to remove both stationary and varying harmonics from the time signals. Cepstral techniques can coincide with OMA by computing the pole and zero part of system transfer function by curve-fitting the liftered response measurements, what can also lead to estimation of frequency response functions, shown in [4]. Otherwise, cepstrally edited measurements can be used with a standard system identification methods for modal parameter computation.

The trio for a semi-automated OMA of rotating machinery proposed in this paper comprise of harmonic detection using a measure of signals kurtosis, harmonic reduction with orthogonal projections of a harmonic realizations of the signal onto the raw signals and estimation of modal parameters of the system with their statistical uncertainties propagated from the measurements. The paper is organized as follows: the next section recalls the methods, subsequently the results are presented in the section 3 and section 4 contains concluding remarks.

2 FRAMEWORK FOR OMA WITH HARMONIC DISTURBANCES

Proposed framework for OMA of rotating machinery contains well-known methods and the concepts familiar to OMA community in general. Following section recalls their main assumptions and provides a brief description of the novel harmonic reduction technique. Examples illustrating the concepts listed in this section are from an experimental setup of a rectangular aluminum plate subjected to both random and harmonic excitations. More description about the experimental data can be found in [5].

2.1 Harmonic detection

Since a distribution of a response of a structural system subjected to a random input is asymptotically Gaussian, the presence of deterministic (harmonic) components in the random inputs can be detected by examining its moments. The fourth moment, namely kurtosis $\gamma(1)$, is a measure of the heaviness of the tail of the distribution and yields $\gamma = 3$ for a normally distributed samples x with zero mean μ and a unit variance σ ,

$$\gamma(x|\mu, \sigma) = \frac{E[(x - \mu)^4]}{\sigma^4} \quad (1)$$

where $E(\cdot)$ is an expectation operator. An illustration of the probability density function from the modal response from an experimental plate subjected to both random and harmonic loads is depicted on Figure 1.

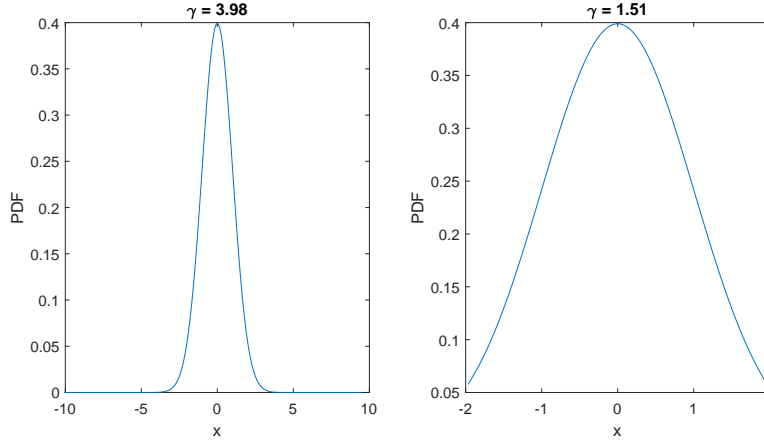


Figure 1: PDF of a predicted structural mode response (left) and a predicted harmonic mode response (right).

The fact that $\gamma \approx 1.5$ for a sinusoidal signals with $\mu = 0$ and $\sigma = 1$ is deployed by Jacobsen et al. [5] in an extended kurtosis check, which is based on extensive calculation of kurtosis of a signal y_i that is bandpass filtered around each examined frequency f_i . Frequencies f_j for which the kurtosis differs from the median computed up to Nyquist frequency are denoted as harmonics. A similar, yet less exhaustive test was proposed by Andersen et al. [6] where only the f_i that exhibits an abrupt change in corresponding singular values (SVs) of power spectral densities (PSDs) of measured channels are tested. The computation of the abrupt change of the SVs is based on a logarithmic metric between current and a median of windowed SVs.

2.2 Harmonic reduction

An application of the orthogonal projection-based algorithm to harmonic reduction was described by Gres et al. [7]. The method follows three steps, namely: a similarity transform of the innovation state space to a modal state space, a prediction of modes that correspond to the harmonic frequencies and an orthogonal projection of raw time series onto the harmonic realization of the output. The algorithm exploits the fact that given a state space system that is completely controllable and observable the subspace-based methods identify all the harmonics as lightly damped modes that can be well predicted and removed by a orthogonal projection onto the subspace spanned by the raw measurements.

The algorithm begins with a similarity transform of the innovation state space model to a modal state space that writes (2a),

$$\hat{z}_{t+1} = (A_0 - K_0 C_0) \hat{z}_t + K_0 y_t \quad (2a)$$

$$\hat{y}_t = C_0 I_m \hat{z}_t \quad (2b)$$

where A_0 , C_0 and K_0 are the state, observation and Kalman gain matrices in a modal form, \hat{z}_t are the modal states and y_t denotes raw time series. The prediction of the modal state space model \hat{y}_t is given by (2b) where I_m is the diagonal selection matrix with ones on a diagonal entries corresponding to harmonic modes. The projection itself is given by (3),

$$E(y_t | \hat{y}_{har}) = y_t - E(y_t \hat{y}_{har}^T) E(\hat{y}_{har} \hat{y}_{har}^T)^{-1} \hat{y}_{har} \quad (3)$$

where \hat{y}_{har} is the predicted harmonic response. The projection yields the reduced, harmonic-free response y_{red} (4),

$$y_{red} = E(y_t | \hat{y}_{har}) \quad (4)$$

To illustrate the concept behind the algorithm, we selected the harmonic frequencies from the experimental plate measurements, namely 374Hz, 748Hz and 1496Hz, for which the prediction of an optimally selected state space model and the projection onto raw measurements were computed, see Figure 2.

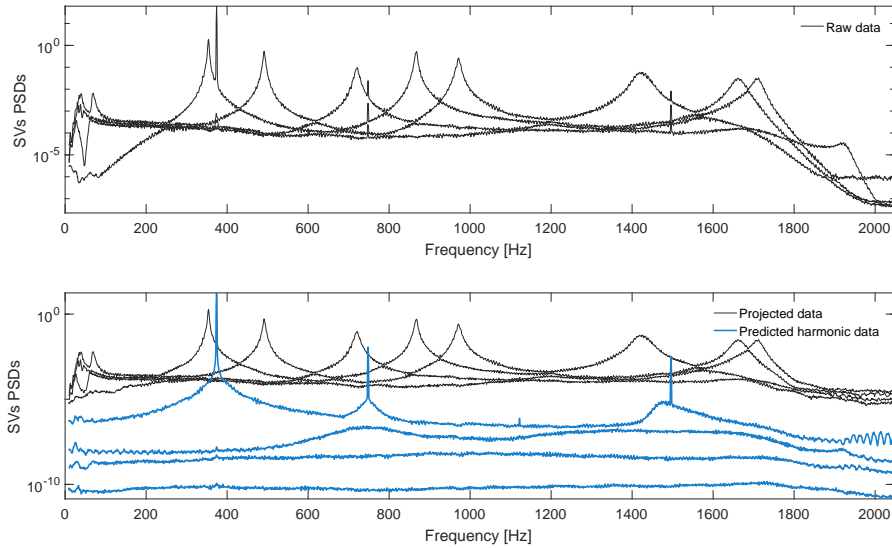


Figure 2: SVs of PSDs from raw, predicted harmonic and projected harmonics-free measurements.

The SVs of the PSDs from the predicted harmonic modes (blue line) match well with the harmonic peaks in the raw measurements, as depicted on Figure 2. The SVs from the data after projection do not contain any artifacts from the orthogonally projected harmonics, hence concluded as harmonic-free.

In general, the principal given by (3) and (4) can be extended not only to harmonic reduction but also to removal of any arbitrary mode from the measurements. That is illustrated based on the same experimental data set from a plate on Figure 3.

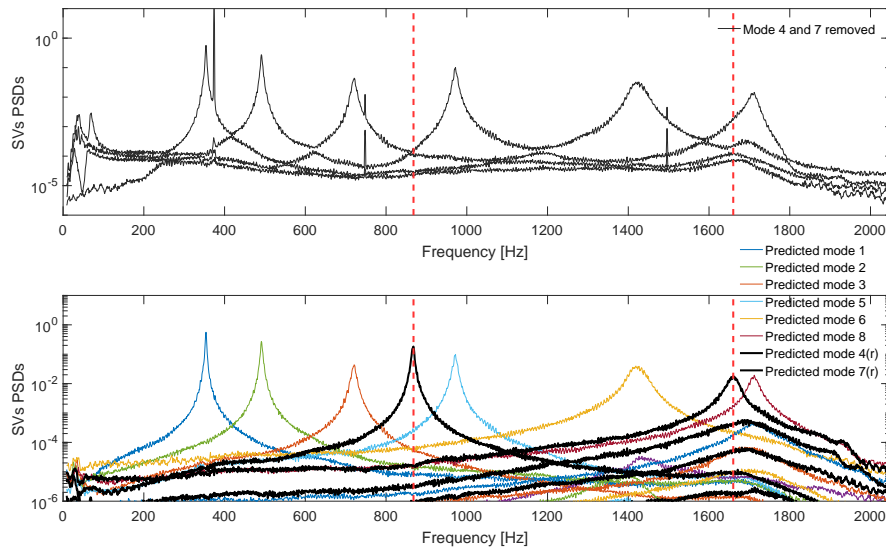


Figure 3: SVs of PSDs from the projected response with mode 4 and 8 removed and predicted responses from each structural mode.

The top subplot of Figure 3 illustrates the SVs of the PSDs from the plate measurements reduced by mode 4 at 868Hz, and mode 8 at 1660Hz. The realization of the modes at 868Hz and 1660Hz is depicted on the bottom part of Figure 3 (thick black lines), along with the complete modal decomposition of the structural modes from the plate measurements. That suggests that any mode can be selected to be reduced in a similar manner.

2.3 Modal parameters computation

The identification of the system matrices of a state space model using both data and covariance driven stochastic subspace identification (SSI-data, SSI-cov) algorithms is subjected to variance errors due to e.g. a finite number of data samples used to calculate the Hankel matrix, unmeasured inputs, measurement noise. A scheme to propagate the sample covariances through all the steps of modal parameter computation for the SSI-cov was proposed by Reynders et al. [8] and Döhler and Mevel [9]. That was extended with SSI-data and input-output algorithms in Mellinger et al. [10].

A method to compute the (co)variance of the modal parameters of the global model order with a data-driven Unweighted Principal Component (UPC) algorithm was developed by Döhler et al. [11]. Method deploys the fast uncertainty computation from [9] and involves computation of the modal parameters of the global mode as a weighted mean of different model orders where the (co)variance of the global model is computed subsequently as a covariance of the weighted mean. The implementation of this algorithm, denoted as SSI with Extended Unweighted Principal Component (UPCX), is used here for the computation of modal parameters and corresponding uncertainties.

3 RESULTS

In the following, we apply presented framework for dealing with harmonics in OMA to an experimental measurements of a full scale ferry during its operation. The analysis is conducted in semi-automatic chain and is illustrated based on the results from a commercial software *ARTEMIS Modal Pro 5.2* [12].

The ferry with its geometrical and mechanical data is presented on Figure 4.



Shipyards:
 Flensburger Schiffbaugesellschaft
 Length over all: 199,8 m
 Ship speed: 22,5 kn
Main engine:
 9L 60 MC-C (MAN B&W, 9 cylinder)
 Power: 20 070 kW
 Nominal rotation speed: 123 rpm
 Working process: two-stroke
Propeller:
 4-bladed with controllable pitch

Figure 4: Full-scale ship docking at Flensburg shipyard.

The dynamic tests are conducted under operational conditions where the response measurements are recorded with piezo-electric accelerometers using a 16-channel B&K Dyn-X acquisition system. The ferry is excited by a combination of a random environmental (wind and waves) and harmonic (operating engine and propeller) loads. The response is measured over a period of 90min and sampled with 128Hz. The measurements were carried out by Dr. Sven-Erik Rosenow, Santiago Uhlenbrock and Prof. Günter Schlottmann from University of Rostock in Germany and made available to analysis by Structural Vibration Solutions A/S from Aalborg, Denmark. The same data set was analyzed in [13] and [14] with respect to harmonic detection and in [7] for harmonic reduction.

Prior to harmonic detection the measurements are detrended, normalized by the standard deviation of each channel and decimated to 21.33Hz. The families of the harmonic frequencies caused by the engine operating at the frequency of 2.05Hz and the propeller blade at 8.2Hz are identified with fast kurtosis check, what is illustrated on the Figures 5 and 6.

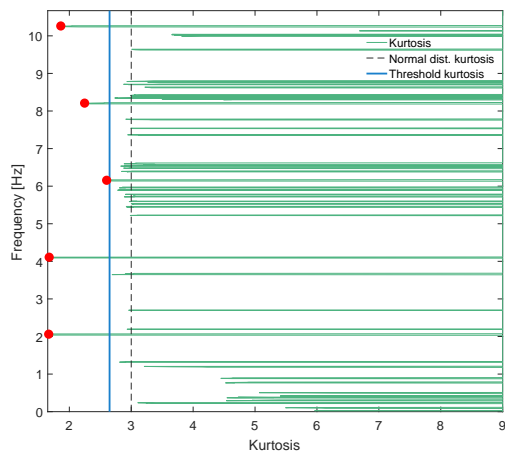


Figure 5: Kurtosis of the signal calculated for the selected frequencies

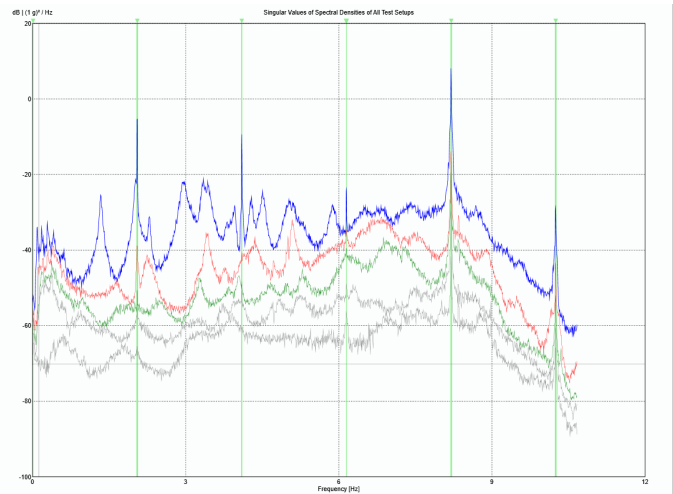


Figure 6: SVs of PSDs with harmonic indicators computed with the fast kurtosis check.

In total five frequencies with the kurtosis below 2.65 are denoted as harmonics, see Figure 5, what is in good agreement with the sharp peaks of SVs depicted on Figure 6. Selected frequencies are one of the input parameters for the orthogonal projection-based harmonic reduction. Besides that, user defined settings boil down to setting a number of block rows of the data Hankel

matrix and a maximum damping ratio of the modes to reduce. Selected parameters navigate the method in finding the optimal state space model to predict the harmonic responses. The input settings with the SVs of PSDs of the measurements before and after the reduction are illustrated on Figure 7.

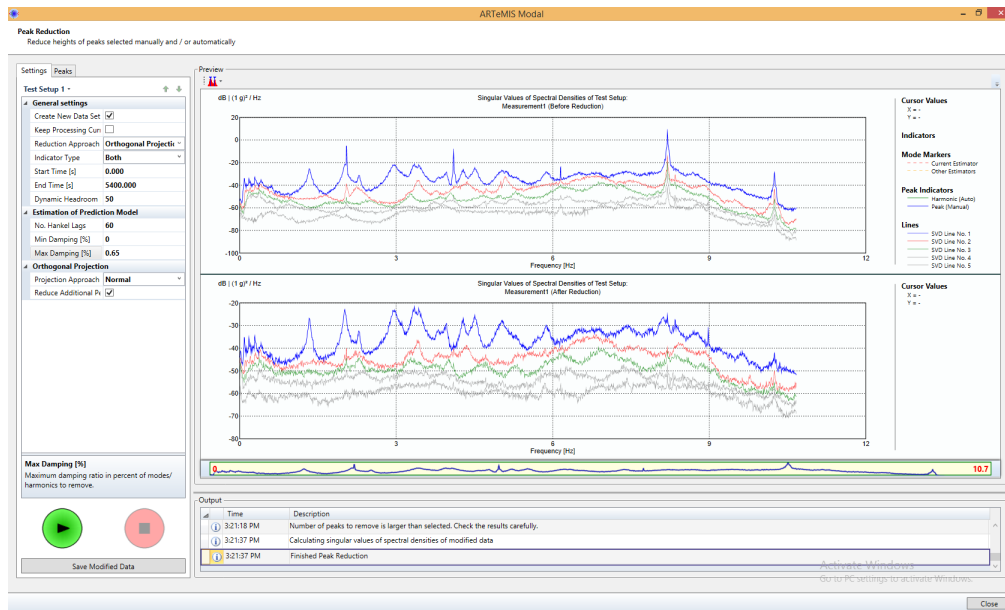


Figure 7: Removal of harmonics at 2.05Hz, 4.1Hz, 6.15Hz, 8.2Hz and 10.2Hz.

Figure 7 illustrates that the harmonic peaks at 2.05Hz, 4.1Hz and 6.15Hz are removed completely. The first SV shows a remanence of the propeller mode at 8.2Hz and the engine mode at 10.2Hz, however both are marginal and not identified during system identification, see Figure 10. The harmonic removal uncovered a mode at 8.14Hz, which being reasonably damped, 1.62%, and with a low complexity, 7.19%, indicates a structural mode close to a resonance with the propeller frequency. To prove the merit of removing the harmonics prior to system identification we conducted a OMA of two data sets before and after harmonic reduction. That is illustrated by the results of the 95% confidence ellipsoids of the 1st mode frequency and damping ratios and the modal assurance criteria (MAC) between the identified sets of mode shapes, see Figures 8 and 9 respectively. The modal parameters from both sets are computed with SSI-UPCX with max. model order of 140 and 38 eigenvalues in the state matrix.

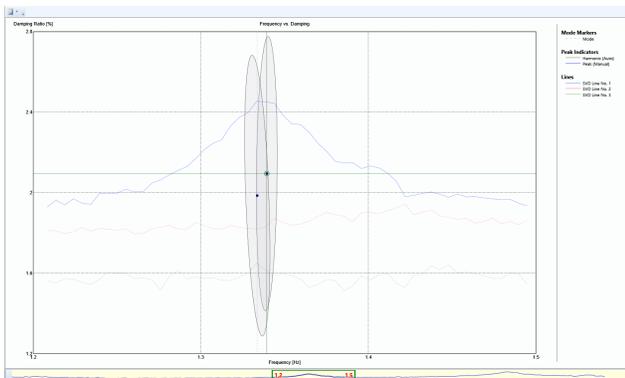


Figure 8: 95% confidence ellipsoids for 1st mode frequency and damping before and after harmonic reduction.

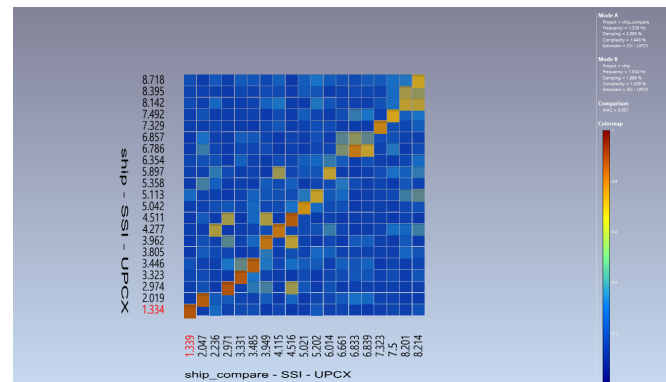


Figure 9: MAC diagram obtained from mode shapes of the system before and after harmonic reduction.

For the global mode estimate, the pairs of the natural frequency and the damping ratio of the 1st mode (unaffected by the harmonics) yields 1.33Hz with 1.99% and 1.34Hz with 2.02%, respectively for the measurements before and after the harmonic reduction. After examining the uncertainty ellipsoids depicted on Figure 8 it becomes apparent that the difference between the modal properties of two modes described above is acceptable hence the mean values from both test are encapsulated within a common uncertainty interval. The diagonal MAC values illustrated on Figure 9 are varying in between 0.75-0.99 suggesting that the modes with similar shapes are computed in both data sets. The modes at 3.8Hz, 5.35Hz, 6.35Hz, 6.86Hz, 8.4Hz and 8.7Hz were not identified before harmonic reduction, see Figure 9. For the completeness of the results a stabilization diagram with corresponding natural frequencies estimated after the harmonic removal is presented on Figure 10.

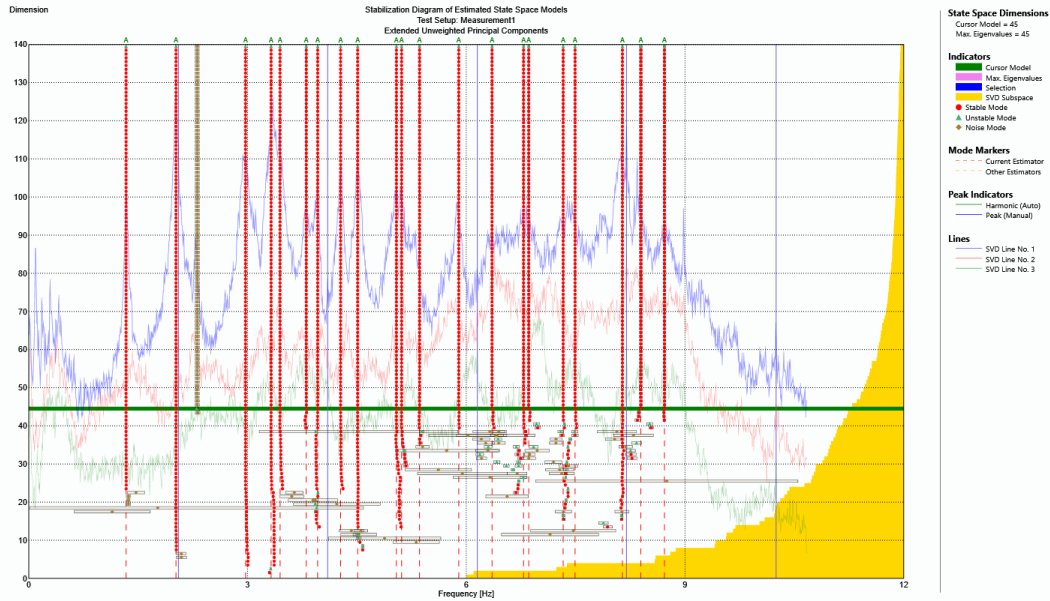


Figure 10: Stabilization diagram of models obtained from data after the harmonic reduction. SSI-UPCX

Figure 10 illustrates multiple stable modes for all the model orders up to 140. One can notice a mode present at 2.29Hz which is denoted as a noise mode- that is a result of a high coefficient of variation of the frequency of the corresponding mode, namely 0.015. Otherwise, the remaining modes present in the measurements exhibit low uncertainties for both the frequency and damping ratio below the threshold being 0.01 and 1 respectively. The harmonic modes previously present in the recorded data are not detected.

4 CONCLUSION

In this paper we presented a semi-automated framework for OMA of rotating machinery. Proposed strategy combines the well-known methods for harmonic detection and modal parameters computation with a novel harmonic reduction technique. Deployed methods operate in time domain, do not require additional inputs for reduction of non-stationary harmonics such as a tachometer measurements and estimate the variance of a global modal parameters, which provides more precise identification of the modal properties in case of realistic applications.

REFERENCES

- [1] Peeters, B., Cornelis, B., Janssens, K. and Van der Auweraer, H., *Removing Disturbing Harmonics in Operational Modal Analysis, Proceedings of the International Operational Modal Analysis Conference, 2007.*
- [2] Combet, F. and Gelman, L., *An automated methodology for performing time synchronous averaging of a gearbox signal*

without speed sensor, Mechanical Systems and Signal Processing, Vol. 21, No. 6, pp. 2590 – 2606, 2007.

- [3] **Randall, R. and Smith, W.**, *New cepstral techniques for operational modal analysis*, *Proceedings of the First World Congress on Condition Monitoring*, 2017.
- [4] **Randall, R., Coats, M. and Smith, W.**, *Repressing the effects of variable speed harmonic orders in operational modal analysis*, Mechanical Systems and Signal Processing, Vol. 79, No. Supplement C, pp. 3 – 15, 2016, special Issue from ICEDyn 2015.
- [5] **Jacobsen, N.-J., Andersen, P. and Brincker, R.**, *Using enhanced frequency domain decomposition as a robust technique to harmonic excitation in operational modal analysis*, *Proceedings of the International Operational Modal Analysis Conference (IOMAC 2007)*, Vol. 4, 01 2007.
- [6] **Andersen, P., Brincker, R., Ventura, C. and Cantieni, R.**, *Estimating Modal Parameters of Civil Engineering Structures subject to Ambient and Harmonic Excitation*, *EVACES - 7th International Conference of Experimental Vibration Analysis for Civil Engineering Structures*, Porto, Portugal, 2007.
- [7] **Gres, S., Andersen, P., Hoen, C. and Damkilde, L.**, *Orthogonal projection-based harmonic signal removal for operational modal analysis*, *IMAC - XXXVI International Modal Analysis Conference*, Orlando, USA, 2018.
- [8] **Reynders, E., Pintelon, R. and Roeck, G. D.**, *Uncertainty bounds on modal parameters obtained from stochastic subspace identification*, Mechanical Systems and Signal Processing, Vol. 22, No. 4, pp. 948 – 969, 2008, special Issue: Crack Effects in Rotordynamics.
- [9] **Döhler, M. and Mevel, L.**, *Fast multi-order computation of system matrices in subspace-based system identification*, *Control Engineering Practice*, Vol. 20, No. 9, pp. 882 – 894, 2012.
- [10] **Mellinger, P., Döhler, M. and Mevel, L.**, *Variance estimation of modal parameters from output-only and input/output subspace-based system identification*, *Journal of Sound and Vibration*, Vol. 379, No. Supplement C, pp. 1 – 27, 2016.
- [11] **Döhler, M., Andersen, P. and Mevel, L.**, *Variance computation of modal parameter estimates from UPC subspace identification*, *IOMAC - 7th International Operational Modal Analysis Conference*, Ingolstadt, Germany, 2017.
- [12] **Structural-Vibration-Solutions**, *ARTeMIS Modal Pro 5.2*, 2017.
- [13] **Jacobsen, N.-J. and Andersen, P.**, *Operational Modal Analysis on Structures with Rotating Parts*, *Proceedings of the International Conference on Noise and Vibration Engineering*, KU Leuven, 2008.
- [14] **Rosenow, S.-E., Uhlenbrock, S. and Schlottmann, G.**, *Parameter Extraction of Ship Structures in Presence of Stochastic and Harmonic Excitations*, *Proceedings of the International Operational Modal Analysis Conference (IOMAC 2007)*, Vol. 4, 01 2007.